Measurements of Surface Diffusivity and Coarsening during Pulsed Laser Deposition

J. D. Ferguson,[1,2] G. Arikan,[3,2] D. S. Dale,[4] A. R. Woll,[4] and J. D. Brock[3,2]

[1]*Department of Materials Science and Engineering, Cornell University, Ithaca, New York 14853, USA*
[2]*Cornell Center for Materials Research, Cornell University, Ithaca, New York 14853, USA*
[3]*School of Applied and Engineering Physics, Cornell University, Ithaca, New York 14853, USA*
[4]*Cornell High Energy Synchrotron Source, Cornell University, Ithaca, New York 14853, USA*

(Received 16 October 2009; published 18 December 2009)

Pulsed laser deposition (PLD) of homoepitaxial $SrTiO_3\langle 001\rangle$ was studied with *in situ* x-ray specular reflectivity and surface diffuse x-ray scattering. Unlike prior reflecivity-based studies, these measurements access both time and length scales of the evolution of the surface morphology during growth. In particular, we show that this technique allows direct measurements of the diffusivity for both inter- and intralayer transport. Our results explicitly limit the possible role of island breakup, demonstrate the key roles played by nucleation and coarsening in PLD, and place an upper bound on the Ehrlich-Schwoebel barrier for downhill interlayer diffusion.

DOI: 10.1103/PhysRevLett.103.256103 PACS numbers: 68.47.Gh, 61.05.cf, 81.15.Fg

Pulsed laser deposition (PLD) presents an exceptional challenge for experimental and theoretical study due to its highly nonequilibrium nature, the vast range of time scales and length scales involved, and the complex stoichiometry of the materials system studied. Consequently, fundamental issues, such as the roles played by the pulsed nature and the kinetic energy of the deposit, remain unresolved [1–5]. System-specific kinetic properties are also difficult to obtain. For example, scanning tunneling microscopy has revealed a rich variety of phenomena on $SrTiO_3$ surfaces [6,7], but at time scales longer than those relevant to growth. In contrast, fast studies of PLD have typically employed electron [2,8] or x-ray [3–5,9,10] specular reflectivity. These studies have excellent time resolution, but are sensitive only to the average atomic-scale surface roughness [11,12], and therefore provide an incomplete description of surface kinetics.

In this Letter, we show that *in situ* x-ray diffuse scattering provides critical length scale information absent from x-ray reflectivity alone, at time scales appropriate to study PLD. The experimental details are given in Ref. [13]. Figures 1(a)–1(c) show false color images of the intensity of both the specular ($q_{||} = 0$) and the surface diffuse scattering as a function of time and $q_{||}$, during the deposition of approximately 11 monolayers (ML) of unit cell step height of $SrTiO_3$ at 3 temperatures. As material is deposited on the surface, the specular intensity drops while diffuse lobes of scattering appear on both sides of the specular rod. These lobes are cuts through ''Henzler rings'' arising from 2D islands on the surface [14,15], as verified by *ex situ* atomic force microscopy (see Ref. [13], Fig. 2).

At low layer coverage, θ ($0 < \theta < 0.4$ ML), the radius of these rings, q_0, is inversely proportional to the average island separation, $L_{\mathrm{isl}} \approx 2\pi/q_0$ [16]. As more material is deposited, the intensity of the specular rod and the diffuse lobes oscillate out of phase with a period of 1 ML. Near layer completion ($0.7 < \theta < 1$ ML), q_0 is a measure of the separation between holes rather than islands.

A feature of Figs. 1(a)–1(c) is that increasing the substrate temperature results in a decrease in q_0, corresponding to a decrease in island density, as expected from classical nucleation theory [17]. A second feature of the data is that q_0 decreases with increasing layer number. This is a general feature of every data set we obtained, and reflects the growth surface's ''memory'' of underlying layers. If a new layer nucleates before layer completion, the remaining holes function as adatom sinks, reducing the adatom density, thereby producing a smaller nucleation density.

Figures 1(d)–1(f) show an enlarged view of the 1st ML of growth from Figs. 1(a)–1(c). At 1000 °C, diffuse scattering appears between the first and second pulses. At sufficiently lower temperatures ($\leq$785 °C), diffuse scattering is not visible until after the second pulse, indicating either delayed nucleation or intensity below our detection limit, as discussed below.

To extract quantitative information, the x-ray data were fit to the sum of three independent components,

$$I_{\mathrm{fit}}(q_{||}) = I_{\mathrm{bg}} + I_{\mathrm{spec}}(q_{||}) + I_{\mathrm{diff}}(q_{||} + q_0) + I_{\mathrm{diff}}(q_{||} - q_0). \tag{1}$$

In this equation, I_{bg} is a constant background, and $I_{\mathrm{spec}}(q_{||})$, $I_{\mathrm{diff}}(q_{||} + q_0)$, and $I_{\mathrm{diff}}(q_{||} - q_0)$ take the form

$$f(x) = I_0/[1 + \xi^2 x^2]^{3/2}, \tag{2}$$

where ξ is the correlation length. The parameters I_0 and ξ each take on two values, associated with I_{spec} and I_{diff}. Equation (2) with $q_0 = 0$ corresponds to the scattering profile of a random distribution of islands [18,19]. Figures 1(g)–1(i) show the single frames from Figs. 1(d)–1(f) corresponding to $t = 16.5$ s: the frame following the third laser pulse. Also shown are the best

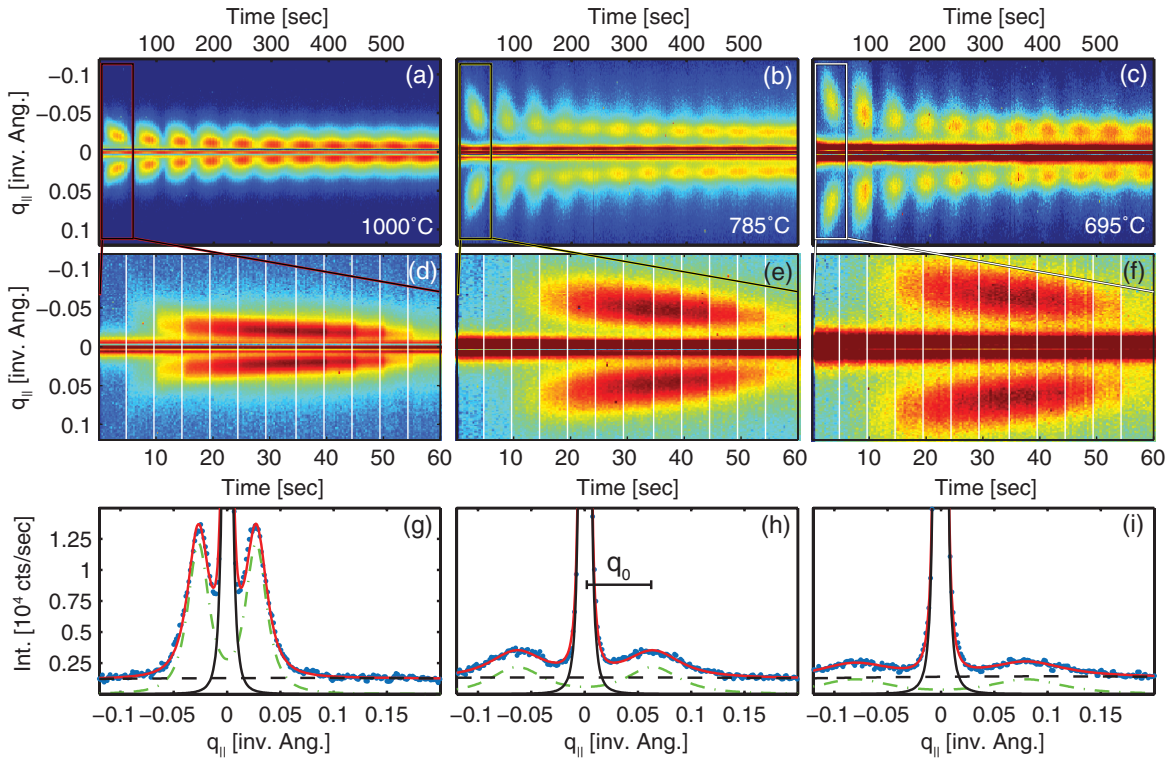

FIG. 1 (color). Diffuse x-ray scattering for the PLD of $SrTiO_3\langle 001\rangle$. (a)–(c) Depositions of ~11 ML at 1000 °C, 790 °C, 695 °C, respectively. (d)–(f) The corresponding first ML. Vertical lines represent the laser pulses (first pulse at 5 s). (g)–(i) Scattering line shape at $t = 16.5$ s for each temperature. I_{fit} (red, solid) consists of I_{diff} (green, dash-dotted), I_{spec} (black, solid), and I_{bg} (black, dashed).

fit to Eq. (1) and its components. The agreement between the fitting function and the data is excellent, with a typical $\chi^2 \approx 1.3$.

Figure 2(a) shows the evolution of q_0 and ξ for the first monolayer at 850 °C. Immediately following the first pulse, a diffuse peak is observed at $q_0 = 0.066 \pm 0.005$ Å, indicating that some islands have nucleated. This value of q_0 corresponds to an island density of $n_x = (1.0 \pm 0.1) \times 10^{12}$ cm^{-2} if a triangular lattice is assumed. A rising q_0 immediately following the first pulse would signify nucleation of new islands from a supersaturation of adatoms. Instead, q_0 decreases monotonically and continuously, indicating a steadily decreasing island density. This shows that some of the newly formed islands are disappearing, and thus that island coarsening [20,21], rather than nucleation, drives the evolution of q_0 during this time. We observe similar coarsening for substrate temperatures as low as 695 °C.

A key parameter in PLD growth is the decay time of the adatom supersaturation resulting from the pulse [22]. Our diffuse scattering measurements are not directly sensitive to adatom supersaturation. Specifically, since they only extend to $q_{\max} = 0.2$ Å^{-1} [see Figs. 1(g)–1(i)], they are insensitive to lateral correlations smaller than $\approx 2\pi/q_{\max} \approx 31$ Å, such as adatoms or very small islands. However, it is easily shown that, if the coverage and specular intensity are both constant, the total diffuse scattering intensity is also constant [23]. We therefore write the total in-plane surface scattering as $I_{\mathrm{tot}} = I_{\mathrm{spec}} + I_{\mathrm{isl}} + I_{\mathrm{sm}}$, where I_{sm} is the scattered intensity from small features not captured by our measurement. I_{isl} is equal to I_{diff} from Eq. (1), integrated over the q_z plane:

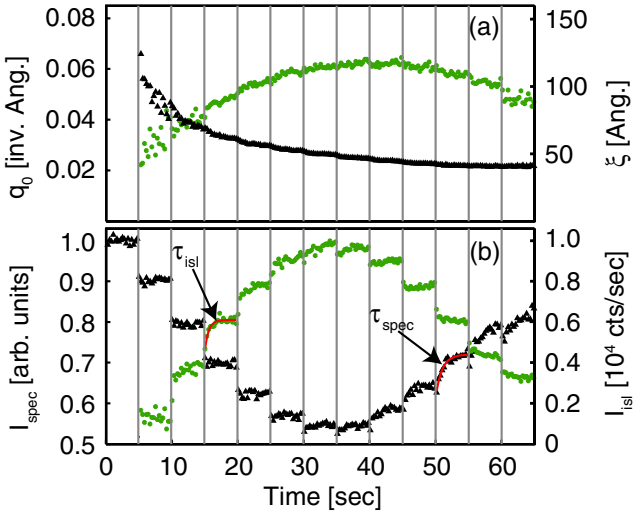

FIG. 2 (color online). (a) The peak position of the diffuse lobes, q_0 (green or gray) and the correlation length, ξ (black) at 850 °C are shown for the first ML. Vertical lines represent laser pulses (first pulse at 5 s). (b) I_{spec} (black) and I_{isl} (green or gray) are shown. The characteristic diffusion times, τ_{isl} and τ_{spec} are determined by fitting I_{spec} and I_{isl}.

$$I_{\mathrm{isl}} = 2\pi I_0(q_0/\xi)[1 + \sqrt{1 + (\xi q_0)^{-2}}], \quad (3)$$

and is associated with the total diffuse scattering due to large islands, i.e., the islands separated by $>2\pi/q_{\max}$. When the specular intensity between pulses is constant, a time-dependent I_{isl} corresponds to mass transfer between small features and the characteristic large islands that give rise to I_{isl}.

The specular intensity I_{spec} and total diffuse intensity I_{isl} for an 850 °C deposition are shown in Fig. 2(b). Apart from the jumps in I_{spec} associated with each deposition pulse, we observe two, distinct slower changes occurring between pulses. The first is a change in I_{spec} that occurs near monolayer completion and has been studied previously [2–5,8]. The second slow change, which manifests in I_{isl} and has not previously been reported, occurs at low coverage. After the third laser pulse, the rise in I_{isl} lags behind the fast drop in I_{spec}. As discussed above, this delay indicates an increase in the amount of material in large islands. Moreover, since I_{spec} is constant during this time, this mass transfer corresponds solely to intralayer transport.

The relaxation kinetics described above can be quantified by fitting I_{spec} at high θ, and I_{isl} at low θ to a simple exponential with characteristic relaxation times τ_{spec} and τ_{isl}. However, the physical process or processes giving rise to these time constants cannot be determined from Fig. 2 alone. For example, the diffusing species may come from preexisting islands; therefore, both τ_{spec} and τ_{isl} may be determined by either the rate of adatom detachment or the rate of surface diffusion. If present, an Ehrlich-Schwoebel (ES) barrier for downhill diffusion would also contribute to τ_{spec}. We are able to resolve this ambiguity by examining the relationship between τ_{spec} and q_0 obtained for different layers in a single growth, exploiting the fact that q_0 decreases with increasing layer number. If diffusion is indeed the rate-limiting process determining τ_{spec} and if the average diffusion length L_D is determined by q_0 then the Einstein relation $L_D^2 = 4D\tau$ applies [25]. We associate each q_0 with an approximate diffusion length $L_D = L_{\mathrm{isl}}/2 = \pi/q_0$ (approximately half the distance between hole centers), and plot L_D^2 vs τ_{spec} in Fig. 3. The values used were obtained from approximately the same exposed coverage $\theta \approx 0.8 \pm 0.04$ at several different thicknesses for each film. A clear linear relationship is observed, so that we may associate the slope in Fig. 3 with the diffusivity D. We also assign τ_{isl} to diffusion-limited transport, since only a subset of the processes responsible for τ_{spec} are involved.

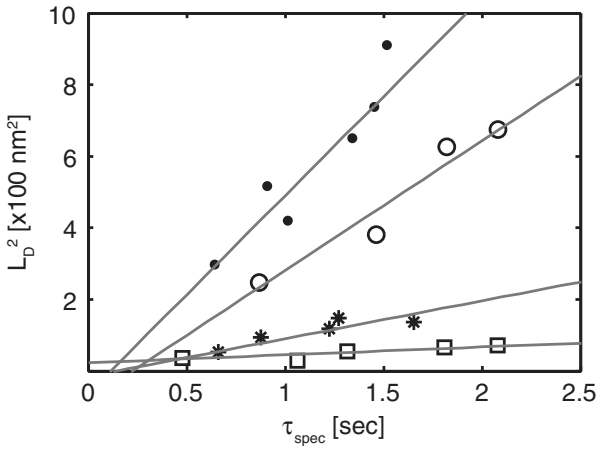

FIG. 3. Length scale for diffusion, L_D^2 vs τ_{spec} for 1000 °C (●), 850 °C (○), 785° (*), and 695 °C (□). The linear relationship shows that diffusion is the rate-limiting process.

Figures 4(a) and 4(b) show Arrhenius plots of D obtained from the analysis of τ_{spec} and τ_{isl} for the first ML. The best-fit lines are shown, corresponding to activation energies of $E_a = 1.0 \pm 0.1$ eV and $E_a = 0.9 \pm 0.2$ eV for inter- and intralayer transport, respectively. The difference in these energies, 0.1 ± 0.22 eV, is a direct measure of the ES barrier. Remarkably, these data sets yield not only the same slopes (within experimental error) but also the same values of diffusivity throughout the temperature range studied, suggesting that the ES barrier is negligible. We thus combine the data in Figs. 4(a) and 4(b) to give the single result $D = D_0 \exp(-E_a/k_B T)$, with $D_0 = 10^{-8\pm1}$ cm^2 s^{-1} and $E_a = 0.97 \pm 0.07$ eV. The determination of both D_0 and E_a through diffraction-based measurements alone represents a principle result of this work.

The value of E_a reported here is larger than 2 values, 0.48 ± 0.05 eV and 0.6 ± 0.2 eV, previously reported [2,10]. In these reports, E_a was obtained from the tempera-

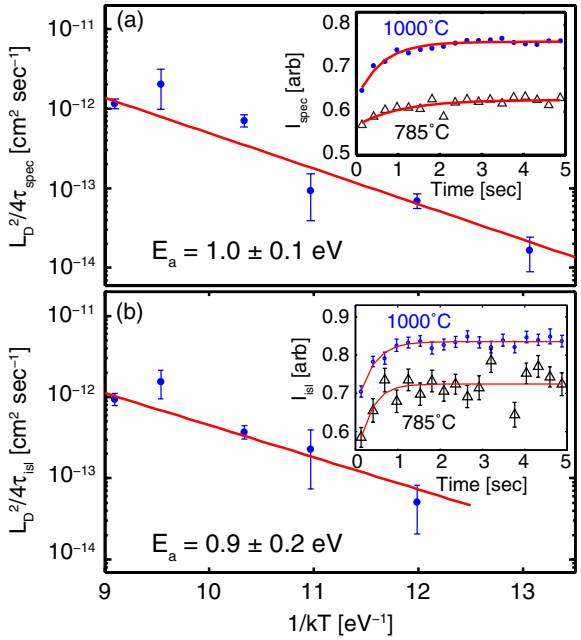

FIG. 4 (color online). (a) Arrhenius behavior of the diffusivity at $\theta \approx 0.8$ ML; (inset) τ_{spec} is obtained from the specular relaxation at high coverage, during interlayer transport. (b) Diffusivity at $\theta \approx 0.25$ ML; (inset) τ_{isl} is determined by fitting the time evolution of I_{isl}.

ture dependence of τ_{spec} implicitly assuming a constant length scale. The effect of this assumption on the determination of E_a is made explicit by writing the temperature dependence of the length scale in Arrhenius form, $L_D = L_0 \exp(-E_L/k_B T)$, and rewriting the Einstein relation

$$\tau_{\mathrm{spec}} = (L_0^2/4D_0)\exp[(E_a - 2E_L)/k_B T]. \quad (4)$$

Equation (4) shows that the activation energy measured from τ_{spec} alone underestimates the activation barrier for diffusion E_a by $2E_L$. We note that our value of $E_a = 0.97 \pm 0.07$ eV is very close to that of 1.2 ± 0.1 eV measured for diffusion of TiO_x ''diline'' units on a reconstructed $SrTiO_3$ surface [7].

Our results provide new insight into the possibility of energetic mechanisms promoting smooth growth in complex-oxide PLD. One such proposed mechanism is island breakup, in which energetic impinging material breaks up existing islands, delaying second-layer nucleation. Island breakup has previously been observed in simulations of metal/metal epitaxy [26,27] and was recently invoked [5] to explain experimental results of PLD of $La_{1-x}Sr_xMnO_3$ on $SrTiO_3$. Specifically, Ref. [5] suggests that island breakup produces an increasing island density when $\theta < 0.5$ ML. Although the system studied here is not precisely the same as in Ref. [5], Fig. 2(a) demonstrates that the island density monotonically decreases with θ from the earliest moments after nucleation. Island breakup could also manifest in our measurement as a decrease in I_{isl} as mass is transferred from large islands to smaller species without changing q_0. However, we do not observe such a decrease. Thus, the possible manifestations of island breakup in our data are obscured by island coarsening.

A second proposed nonthermal smoothing mechanism suggested by prior experimental work on complex-oxide PLD, is enhanced downhill transport [2–5]. The experimental basis for this suggestion is the observation, based on specular reflectivity, that downhill transport occurs on two widely separated time scales [3,4]. Our observation, that island nucleation occurs quickly, followed by coarsening, suggests an alternate origin of these two time scales. Specifically, it is possible that the mobile species responsible for slow downhill transport consists of material that detaches from islands. This material need not be chemically identical with the species arriving from the plume. Interestingly, we note that the prefactor reported here, $D_0 = 10^{-8\pm1}$ cm^2 s^{-1}, is 5 orders of magnitude lower than typical experimental and theoretical value for metal and semiconductor systems [28]. Similar diminished prefactors have previously been associated with correlated motion involving multiple atoms [28]. Here, it might be associated with stoichiometric mass transfer of Sr-containing and Ti-containing species.

In summary, we have presented time-resolved x-ray reflectivity and diffuse scattering measurements obtained during PLD. Our results constitute direct observations of island nucleation as little as 200 ms after the pulse, and direct evidence of island coarsening occurring between laser pulses for temperatures as low as 695 °C. Quantitative analysis of our results allow us to independently estimate the inter- and intralayer diffusivity (prefactor and activation barrier) of mobile species between pulses and to place an upper bound on the ES barrier. Our measurements significantly impact prior estimates of the thermal diffusivity involved in $SrTiO_3$ growth, and place specific constraints on energetic smoothing mechanisms that have been proposed to occur during PLD.

We thank J. Blakely, Y. Kim, H. Wang, D. Muller, and M. Tate. This research was conducted in part at the Cornell High Energy Synchrotron Source and was supported by NSF (DMR-0317729 and DMR-0225180).

[1] M. Aziz, Appl. Phys. A **93**, 579 (2008).
[2] D. H. A. Blank *et al.*, Appl. Phys. A **69**, S17 (1999).
[3] A. Fleet *et al.*, Phys. Rev. Lett. **94**, 036102 (2005).
[4] J. Tischler *et al.*, Phys. Rev. Lett. **96**, 226104 (2006).
[5] P. R. Willmott *et al.*, Phys. Rev. Lett. **96**, 176102 (2006).
[6] M. Lippmaa *et al.*, Appl. Surf. Sci. **130–132**, 582 (1998).
[7] H. L. Marsh *et al.*, Nanotechnology **17**, 3543 (2006).
[8] M. Lippmaa *et al.*, Appl. Phys. Lett. **76**, 2439 (2000).
[9] D. Dale *et al.*, Phys. Rev. B **74**, 085419 (2006).
[10] A. Fleet *et al.*, Phys. Rev. Lett. **96**, 055508 (2006).
[11] S. K. Sinha *et al.*, Phys. Rev. B **38**, 2297 (1988).
[12] D. Dale, Y. Suzuki, and J. D. Brock, J. Phys. Condens. Matter **20**, 264008 (2008).
[13] See EPAPS Document No. E-PRLTAO-104-010001 for experimental details. For more information on EPAPS, see http://www.aip.org/pubservs/epaps.html.
[14] P. Hahn, J. Clabes, and M. Henzler, J. Appl. Phys. **51**, 2079 (1980).
[15] M. C. Bartelt and J. W. Evans, Surf. Sci. **298**, 421 (1993).
[16] E. Dulot, B. Kierren, and D. Malterre, Thin Solid Films **423**, 64 (2003).
[17] H. Brune *et al.*, Phys. Rev. B **60**, 5991 (1999).
[18] P. Debye, H. R. Anderson, and H. Brumberger, J. Appl. Phys. **28**, 679 (1957).
[19] R. N. Bracewell, *The Fourier Transform and Its Applications* (McGraw-Hill, Boston, 2000), 3rd ed.
[20] N. C. Bartelt, W. Theis, and R. M. Tromp, Phys. Rev. B **54**, 11 741 (1996).
[21] J. M. Wen *et al.*, Phys. Rev. Lett. **76**, 652 (1996).
[22] P. O. Jubert, O. Fruchart, and C. Meyer, Surf. Sci. **522**, 8 (2003).
[23] By integrating Eq. (6) in Ref. [24] over $q_{||}$, it is seen that both I_{spec} and I_{diff} depend only on $h(q_z)$, the Fourier transform of the vertical height distribution.
[24] S. K. Sinha *et al.*, Physica (Amsterdam) **231A**, 99 (1996).
[25] R. Gomer, Rep. Prog. Phys. **53**, 917 (1990).
[26] J. Jacobsen, B. H. Cooper, and J. P. Sethna, Phys. Rev. B **58**, 15 847 (1998).
[27] J. M. Pomeroy *et al.*, Phys. Rev. B **66**, 235412 (2002).
[28] E. Kaxiras and J. Erlebacher, Phys. Rev. Lett. **72**, 1714 (1994).